

Recent quarkonium results from Belle II

R. Garg on behalf of the Belle II collaboration^{a,*}

^aCarnegie Mellon University,

5000 Forbes Avenue, Pittsburgh, USA

E-mail: renu2@andrew.cmu.edu

The Belle II experiment at the SuperKEKB energy-asymmetric e^+e^- collider is the upgraded successor of the B -factory facility at the KEK laboratory, Japan. The designed instantaneous luminosity of the machine is $6 \times 10^{35} \text{cm}^{-2}\text{s}^{-1}$. The Belle II experiment aims to ultimately accumulate 50ab^{-1} of data, 50 times more than its predecessor. The first data taking period beyond the $\Upsilon(4S)$ peak energy has been devoted to the study of the region around $\sqrt{s} = 10.75$ GeV, where enhanced transition rates to lower bottomonia suggested the existence of a new exotic bound state. This proceedings summarizes the most recent measurements of exotic quarkonium states to probe the fundamentals of QCD at the Belle II experiment.

XVI International Conference on Heavy Quarks and Leptons (HQL 2023)
November 28, 2023 to December 2, 2023
TIFR, Mumbai, India

*Supported by U. S. Dept. of Energy under contract number DE-SC-0010118

7 1. Introduction

8 Heavy quarkonium spectroscopy offers multiple opportunities to investigate the non-perturbative
 9 behavior of quantum chromodynamics. In recent years various collaborations, in particular those
 10 working at e^+e^- colliders, discovered a number of unexpected quarkonium-like states, labeled as
 11 X , Y , and Z states, in both the charmonium and bottomonium mass regions. Since these exotic
 12 hadrons are not predicted by the quark model, different compositions are being considered, such
 13 as compact tetraquarks, mesonic molecules and hybrids. More experimental results are needed in
 14 this sector for a better understanding of the phenomenology of quarkonium(-like) states and their
 15 transitions.

16 2. $\Upsilon(10753)$ state

17 The $\Upsilon(10753)$ bottomonium-like vector state was observed in the cross-section for the process
 18 of $e^+e^- \rightarrow \pi^+\pi^-\Upsilon(nS)$ ($n = 1, 2, 3$) by Belle [1] and in fits to the $e^+e^- \rightarrow b\bar{b}$ cross-sections at
 19 energies \sqrt{s} from 10.52 to 11.02 GeV [2]. The mass and width of this state are $M = (10753 \pm$
 20 $6) \text{ MeV}/c^2$ and $\Gamma = (36_{-12}^{+18}) \text{ MeV}$, respectively. This mass is not consistent with any of the predicted
 21 states, which makes it difficult to assign the $\Upsilon(10753)$ as a conventional bottomonium state. The
 22 unknown nature of the $\Upsilon(10753)$ state is generating a wide interest on the theoretical side. As the
 23 newly observed state does not correspond to any pure $b\bar{b}$ resonance, the most popular interpretations
 24 describe the $\Upsilon(10753)$ as a mixture of $\Upsilon(4S)$ and $\Upsilon(3D)$ states [3, 4]. Several other interpretations
 25 consider the state as a conventional bottomonium [5–10], hybrid [11], hadronic molecule with
 26 a small admixture of a bottomonium [12], or tetraquark state [13, 14], but there is no definitive
 27 explanation so far.

28 Further measurements of the properties and decay modes of the $\Upsilon(10753)$ are important to
 29 advance our understanding of its nature and test theoretical predictions. Therefore, to confirm
 30 the existence of this new state and study its properties, Belle II performed an energy scan in the
 31 proximity of the $\Upsilon(10753)$, collecting 19.3 fb^{-1} at the four center-of-mass (c.m.) energy points \sqrt{s}
 32 $= 10.653, 10.701, 10.745, 10.805 \text{ GeV}$.

33 2.1 Study of $\Upsilon(10753) \rightarrow (\pi^+\pi^-\pi^0)\gamma\Upsilon(1S)$

34 One interpretation of the $\Upsilon(10753)$ as an admixture of $\Upsilon(4S)$ and $\Upsilon(3D)$ states predicts
 35 comparable branching fractions of 10^{-3} for $\Upsilon(10753) \rightarrow \omega\chi_{bJ}$ and $\Upsilon(10753) \rightarrow \pi^+\pi^-\Upsilon(nS)$.
 36 Also, the branching fraction for $\Upsilon(10753) \rightarrow \omega\chi_{b1}$ is expected to be about 1/5 of that for
 37 $\Upsilon(10753) \rightarrow \omega\chi_{b2}$ [7]. In addition, the process $\Upsilon(10753) \rightarrow \gamma X_b$, $X_b \rightarrow \omega\Upsilon(1S)$, which
 38 shares the same final states as $\Upsilon(10753) \rightarrow \omega\chi_{bJ}$, provides access to the X_b . The X_b is the
 39 bottomonium analogue of the $X(3872)$. Its existence has been predicted in molecular [15–17] and
 40 tetraquark models [18–20].

41 The reaction $e^+e^- \rightarrow \gamma\omega\Upsilon(1S)$ is quite promising because it can result from two of the above-
 42 mentioned decay modes: the $\omega\chi_{bJ}$ transition and the search for the bottomonium analogue of the
 43 $X(3872)$, which is expected to decay to $X_b \rightarrow \omega\Upsilon(1S)$.

44 A significant $\omega\chi_{b1}$ signal and evidence for the $e^+e^- \rightarrow \omega\chi_{b2}$ process at $\sqrt{s} = 10.745 \text{ GeV}$
 45 are found. The corresponding Born cross sections are $(3.6 \pm 0.7 \pm 0.5) \text{ pb}$ and $(2.8_{-1.0}^{+1.2} \pm 0.4) \text{ pb}$.

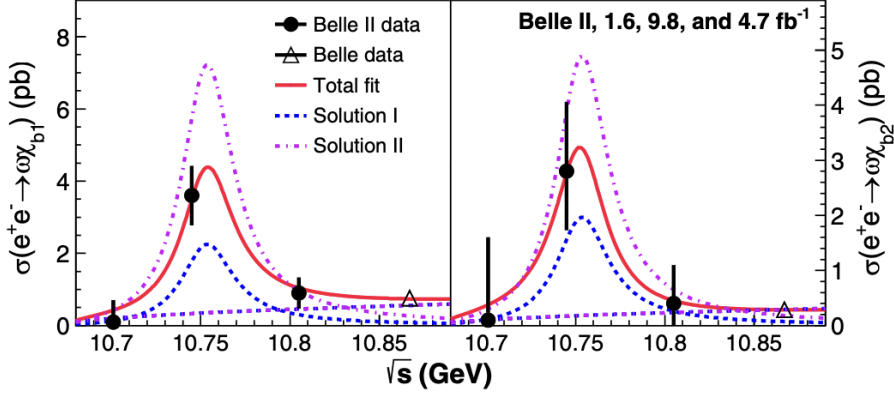


Figure 1: Energy dependence of the Born cross sections for $e^+e^- \rightarrow \omega\chi_{b1}$ (left) and $e^+e^- \rightarrow \omega\chi_{b2}$ (right). Circles show our measurements and triangles are the results of the Belle experiment [22]. Error bars represent combined statistical and systematic uncertainties. Curves show the fit results and various components of the fit function, where the two solutions correspond to the two signs of interference.

46 The Born cross sections for $e^+e^- \rightarrow \omega\chi_{b1}$ and $e^+e^- \rightarrow \omega\chi_{b2}$ as functions of collision energy are
 47 shown in Fig. 1. We observe a strong enhancement of the cross section near 10.75 GeV whose
 48 energy dependence is consistent with the $\Upsilon(10753)$ state.

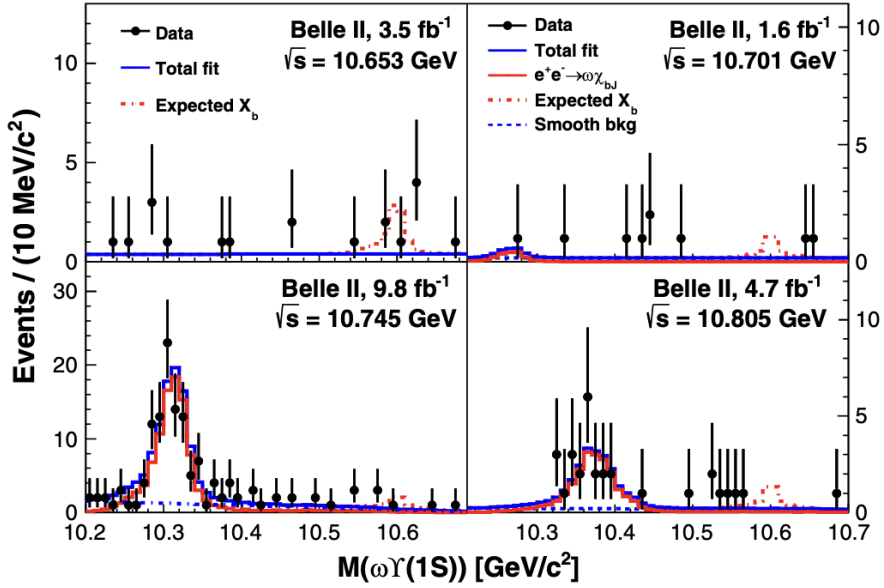


Figure 2: Distributions of $\omega\Upsilon(1S)$ mass from data at $\sqrt{s} = 10.653, 10.701, 10.745,$ and 10.805 GeV. The red dash-dotted histograms are from simulated events $\Upsilon(10753) \rightarrow \gamma X_b, X_b \rightarrow \omega\Upsilon(1S)$ with the X_b mass fixed at $10.6 \text{ GeV}/c^2$ and yields fixed at the upper limit values. The red solid line is the reflection of the $e^+e^- \rightarrow \omega\chi_{bJ}$ signals.

49 We also measured the ratio $\sigma_B(e^+e^- \rightarrow \omega\chi_{b1})/\sigma_B(e^+e^- \rightarrow \omega\chi_{b2}) = 1.3 \pm 0.6$ at $\sqrt{s} = 10.745$
 50 GeV, where the statistical uncertainties and systematic uncertainties are included. This observed

ratio contradicts the expectation for a pure D -wave bottomonium state of 15 [21] and there is also a 1.8σ difference with the prediction of 0.2 for a $S - D$ mixed state [7].

The distributions of $M[\omega\Upsilon(1S)]$ for events within $0.70 < M(\pi^+\pi^-\pi^0) < 0.86$ GeV/ c^2 at $\sqrt{s} = 10.653, 10.701, 10.745,$ and 10.805 GeV are shown in Fig. 2. The reflections of the $e^+e^- \rightarrow \omega\chi_{bJ}$ signals are observed, but no evidence of a X_b signal is obtained for X_b masses between 10.45 and 10.65 GeV/ c^2 . The upper limits at 90% Bayesian confidence on the products of Born cross section for $e^+e^- \rightarrow \gamma X_b$ and branching fraction for $X_b \rightarrow \omega\Upsilon(1S)$ are set to be 0.55, 0.84, 0.14, and 0.37 pb at 10.653, 10.701, 10.745, and 10.805 GeV, respectively.

2.2 Study of $\Upsilon(10753) \rightarrow \omega\chi_{b0}(1P)/\omega\eta_b(1S)$

We next report on a search for the processes $e^+e^- \rightarrow \omega\eta_b(1S)$ and $e^+e^- \rightarrow \omega\chi_{b0}(1P)$ at a c.m. energy of 10.745 GeV, which is close to the peak of the $\Upsilon(10753)$ state. The $\eta_b(1S)$ and $\chi_{b0}(1P)$ mesons do not have exclusive decay channels with a large product of efficiency and branching fraction. Thus, we reconstruct only an ω meson in the $\pi^+\pi^-\pi^0$ decay and use recoil mass,

$$M_{\text{recoil}}(\pi^+\pi^-\pi^0) = \sqrt{\left(\frac{\sqrt{s} - E_\omega}{c^2}\right)^2 - \left(\frac{p_\omega}{c}\right)^2} \quad (1)$$

as the signal extraction variable, where E_ω and p_ω are the energy and momentum of the $\pi^+\pi^-\pi^0$ combination in the c.m. frame. In a previous study [23], we searched for the process $e^+e^- \rightarrow \omega\chi_{b0}(1P)$ fully reconstructing the $\chi_{b0}(1P) \rightarrow \gamma\Upsilon(1S)$ decay and found no significant signal. The probability of the decay $\chi_{b0}(1P) \rightarrow \gamma\Upsilon(1S)$ is small, thus, the sensitivity of partial reconstruction, applied in this analysis, might be higher than that of full reconstruction.

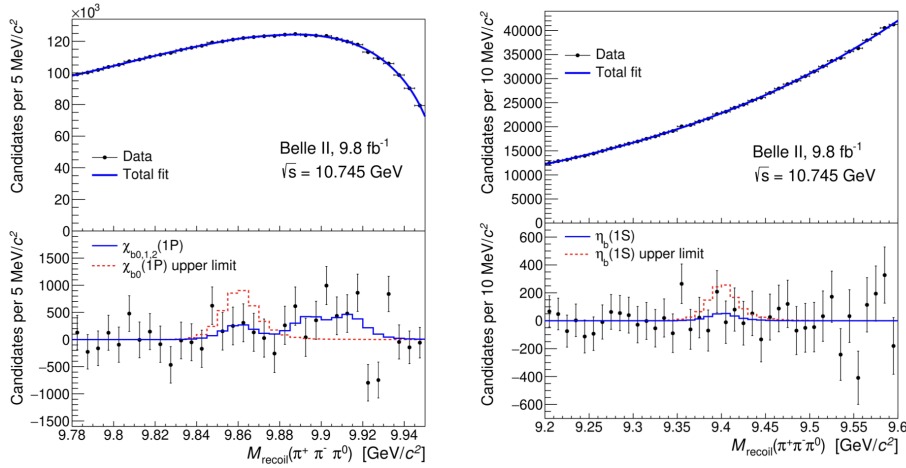


Figure 3: Distribution of $M_{\text{recoil}}(\pi^+\pi^-\pi^0)$ for the $e^+e^- \rightarrow \omega\eta_b(1S)$ (left) and $e^+e^- \rightarrow \omega\chi_{b0}(1P)$ (right) candidates. Top distributions are data points with the fit function overlaid and the bottom are the same distributions with the background component of the fit function subtracted. The solid histogram shows the fit function for the best fit; the dashed histogram shows the same function with the yield fixed to the upper limit.

The fit results of the $M_{\text{recoil}}(\pi^+\pi^-\pi^0)$ for the $e^+e^- \rightarrow \omega\eta_b(1S)$ and $e^+e^- \rightarrow \omega\chi_{b0}(1P)$ decays are shown in Fig. 3. No significant signals are observed. Therefore, we set the 90% confidence

72 level upper limits on the Born-level cross sections:

$$\sigma_B(e^+e^- \rightarrow \omega\eta_b(1S)) < 2.5 \text{ pb,}$$

73

$$\sigma_B(e^+e^- \rightarrow \omega\chi_{b0}(1P)) < 8.7 \text{ pb.}$$

74 The upper limit on the $e^+e^- \rightarrow \omega\chi_{b0}(1P)$ cross section is comparable to the upper limit
 75 obtained using full reconstruction of 11.3 pb [23]. The tetraquark model [13] predicts that
 76 the decay rate of $\Upsilon(10753) \rightarrow \omega\eta_b(1S)$ is strongly enhanced compared to the decay rates of
 77 $\Upsilon(10753) \rightarrow \pi^+\pi^-\Upsilon(nS)$. The obtained upper limit on $\sigma_B(\omega\eta_b(1S))$ is close to the measured
 78 values of $\sigma_B(\pi^+\pi^-\Upsilon(nS))$, which are in the range (1 – 3) pb [1]. Thus, our results do not support
 79 the tetraquark-model prediction that the $\Upsilon(10753) \rightarrow \omega\eta_b(1S)$ decay is enhanced [13]. In the
 80 $4S - 3D$ mixing model, the decay rate of $\Upsilon(10753) \rightarrow \omega\eta_b(1S)$ is smaller than the decay rate
 81 of $\Upsilon(10753) \rightarrow \pi^+\pi^-\Upsilon(nS)$ by a factor 0.2 – 0.4 [24]; our upper limit does not contradict this
 82 expectation.

83 The upper limit on the $\omega\chi_{b0}(1P)$ cross section is higher than the measured $\omega\chi_{b1}(1P)$ and
 84 $\omega\chi_{b0}(1P)$ cross sections of (3.6 ± 0.9) pb and (2.8 ± 1.3) pb, respectively [23]. For a $4S - 3D$ mixed
 85 state, the decay rate to $\omega\chi_{b0}(1P)$ is expected to be comparable to the decay rates to $\omega\chi_{b1}(1P)$ and
 86 $\omega\chi_{b2}(1P)$ [8]; our upper limit is consistent with this expectation. In the charmonium sector, the
 87 decay of the $Y(4230)$ state to $\omega\chi_{c0}$ is enhanced compared to the decays to $\omega\chi_{c1}$ and $\omega\chi_{c2}$ [25].
 88 We do not find an analogous enhancement in the decay pattern of $\Upsilon(10753)$, which may indicate
 89 that the $Y(4230)$ and $\Upsilon(10753)$ have different structures.

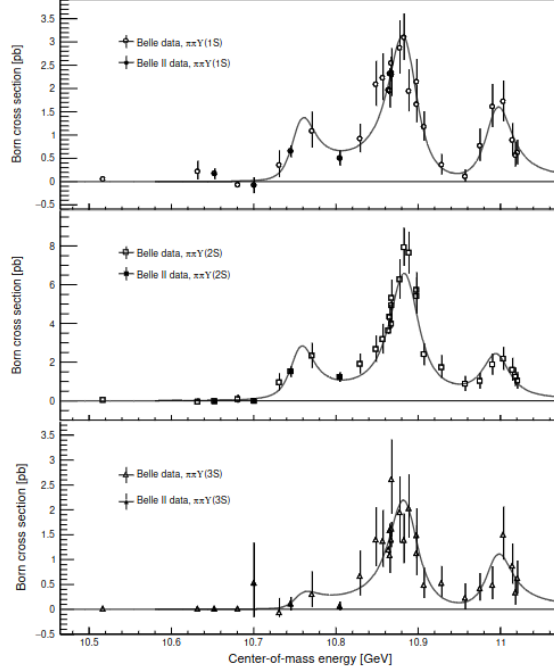


Figure 4: Born cross sections for $\pi^+\pi^-\Upsilon(1S)$ (top), $\pi^+\pi^-\Upsilon(2S)$ (middle), and $\pi^+\pi^-\Upsilon(3S)$ (bottom), with fit results overlaid.

90 2.3 Study of $\Upsilon(10753) \rightarrow \pi^+\pi^-\Upsilon(nS)$

91 We present an analysis of $\Upsilon(10753) \rightarrow \pi^+\pi^-\Upsilon(nS)$ using new, large samples of data collected
 92 explicitly for this purpose by the Belle II experiment. We reconstruct decays to the $\pi^+\pi^-\Upsilon(nS)$
 93 final state, with $\Upsilon(nS)$ decaying to a $\mu^+\mu^-$ pair, at \sqrt{s} from 10.6–10.8 GeV. We calculate and fit the
 94 Born cross sections, σ_B , for these processes as a function of \sqrt{s} to measure the $\Upsilon(10753)$ mass and
 95 width. We also search for intermediate states to study the internal decay dynamics (e.g., $e^+e^- \rightarrow$
 96 $f_0(980)[\rightarrow \pi^+\pi^-]\Upsilon(nS)$) and exotic states ($e^+e^- \rightarrow \pi^\pm Z_b(10610, 10650)^\pm [\rightarrow \pi^\pm \Upsilon(nS)]$), which
 97 may provide deeper understanding into the possibility of an unconventional nature for the $\Upsilon(10753)$.

98 The Born cross sections and the fit to their energy dependence are displayed in Fig. 4. Signals
 99 for the $\Upsilon(10753)$ are observed in $\pi^+\pi^-\Upsilon(1S)$ and $\pi^+\pi^-\Upsilon(2S)$ with greater than 8σ significance,
 100 while no evidence is found for $\pi^+\pi^-\Upsilon(3S)$.

101 The cross-section ratios $\sigma(\pi^+\pi^-\Upsilon(1S, 3S))/\sigma(\pi^+\pi^-\Upsilon(2S))$ at the $\Upsilon(10753)$ resonance peak
 102 are determined for the first time. The values are $0.46^{+0.15}_{-0.12}$ and $0.10^{+0.05}_{-0.04}$ for $\pi^+\pi^-\Upsilon(1S)$ and
 103 $\pi^+\pi^-\Upsilon(3S)$, respectively. The ratio for $\pi^+\pi^-\Upsilon(1S)$ is compatible with the ratios at the $\Upsilon(5S)$ and
 104 $\Upsilon(6S)$ resonance peaks. However, the relative ratio of $\pi^+\pi^-\Upsilon(3S)$ at the $\Upsilon(10753)$ peak is about
 3–4 times smaller than those at the $\Upsilon(5S)$ and $\Upsilon(6S)$ peaks.

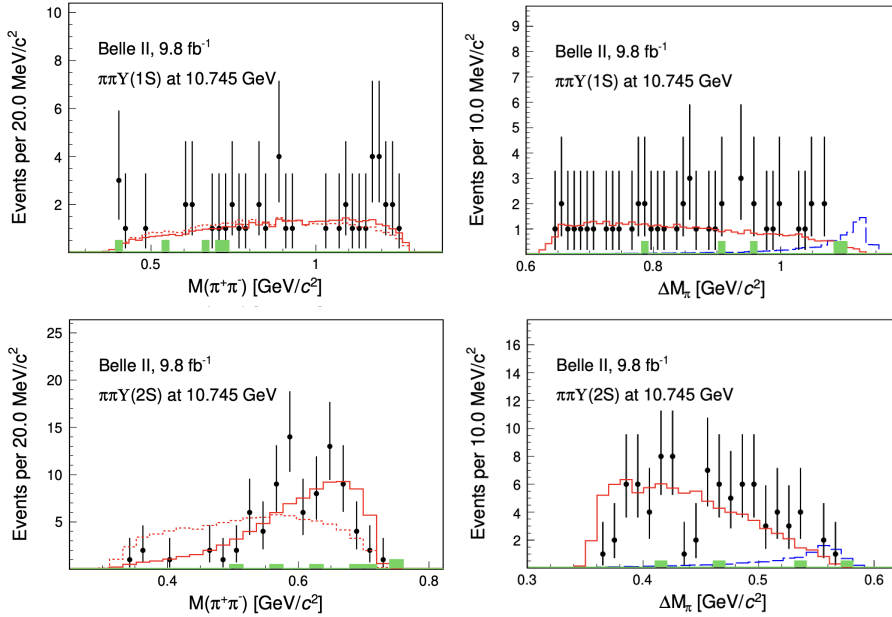


Figure 5: Distributions of dipion mass (left) and maximal difference between the $\pi^+\pi^-\mu^+\mu^-$ mass and the $\pi^\pm\mu^+\mu^-$ mass (right). Plots from top to bottom show $\pi^+\pi^-\Upsilon(1S)$ and $\pi^+\pi^-\Upsilon(2S)$ at $\sqrt{s} = 10.745$ GeV, respectively. Points with error bars show the events in the signal region from data, green shaded histograms show the events in the sideband region, red histograms the weighted simulated signal, red dotted histogram is the phase space signal MC simulation, and blue dashed histogram is the $Z_b(10610, 10650)^\pm$ from MC simulation.

105

106 The distributions of $M(\pi^+\pi^-)$ (left) and ΔM_π (right) for events in the signal regions are shown
 107 in Fig. 5, compared with the events from sideband regions. We did not find any evidence that
 108 these transitions occur via intermediate $Z_b(10610, 10650)^\pm$ states. The dipion invariant mass in

109 $\pi^+\pi^-\Upsilon(1S)$ (Fig. 5, top-left) is consistent with the simulated phase-space distribution. The dipion
 110 invariant mass in $\pi^+\pi^-\Upsilon(2S)$ (Fig. 5, bottom-left) production is similar to that observed in the
 111 $\Upsilon(2S) \rightarrow \pi^+\pi^-\Upsilon(1S)$ process and can be described accurately by the $\Upsilon(nS)$ transition amplitude.
 112 This distribution can provide an input for theoretical calculations.

113 The mass and width of $\Upsilon(10753)$ are measured to be $(10756.3 \pm 2.7 \pm 0.6)$ MeV/ c^2 and
 114 $(29.7 \pm 8.5 \pm 1.1)$ MeV, respectively, which are consistent with previous measurements but with
 115 uncertainties nearly a factor of two smaller. These results supersede the previous Belle result [1].
 116 This improvement in accuracy provides a more precise comparison for theoretical calculations.

117 3. Energy dependence of $e^+e^- \rightarrow B^{(*)}\bar{B}^{(*)}$ cross-section

118 These open-flavor final states, $B^{(*)}\bar{B}^{(*)}$, are expected to be the dominant decay channels for
 119 $b\bar{b}$ hadrons and constitute the main contribution to the total $b\bar{b}$ cross section. Thus, measuring
 120 the exclusive $e^+e^- \rightarrow B^{(*)}\bar{B}^{(*)}$ cross sections provides important information on the interactions
 121 in this energy region and in particular about the structure of bottomonium(-like) resonances. The
 122 measured cross sections can be used in the coupled channel analysis of all available scan data to
 123 extract the parameters of the $b\bar{b}$ states. This topic is of special interest since all the states above
 124 threshold exhibit anomalies, especially in transitions to lower bottomonia, which currently are not
 125 well understood. The analysis follows the analogous measurement performed at Belle [26], where
 the measured energy dependencies of $\sigma(e^+e^- \rightarrow B^{(*)}\bar{B}^{(*)})$ showed an oscillatory behavior.

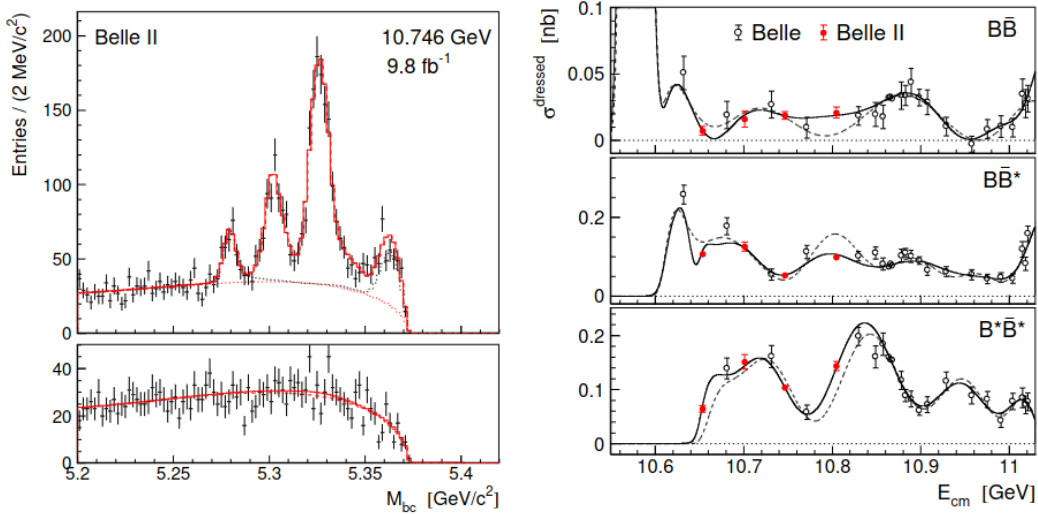


Figure 6: Results of the measurement of the $e^+e^- \rightarrow B\bar{B}$, $e^+e^- \rightarrow B\bar{B}^*$, and $e^+e^- \rightarrow B^*\bar{B}^*$ cross sections using the Belle II scan data. The signal yields are obtained by fitting the M_{bc} distributions (left) at each value of \sqrt{s} and the energy dependence of the Born cross section (right), combined with the measurement from Belle.

126

127

128 In this paper, we report the measurement of the energy dependence of the $e^+e^- \rightarrow B\bar{B}$,
 129 $e^+e^- \rightarrow B\bar{B}^*$, and $e^+e^- \rightarrow B^*\bar{B}^*$ exclusive cross sections. Our approach is to perform a full
 reconstruction of one B meson in hadronic channels, and then to identify the $B\bar{B}$, $B\bar{B}^*$, and $B^*\bar{B}^*$
 130 signals using the M_{bc} distribution, $M_{bc} = \sqrt{(E_{cm}/2)^2 - p_B^2}$, where E_{cm} is the c.m. energy and

131 p_B is the B -candidate momentum measured in the c.m. frame. The M_{bc} distribution for $B\bar{B}$ events
 132 peaks at the nominal B -meson mass, m_B , while the distributions for $B\bar{B}^*$, and $B^*\bar{B}^*$ events peak
 133 approximately at $m_B - \Delta m_{B^*}/2$ and $m_B - \Delta m_{B^*}$, respectively, where Δm_{B^*} is the mass difference
 134 of the B^* and B mesons. The M_{bc} distribution obtained at $\sqrt{s} = 10.746$ GeV is shown in Fig. 6 left.

135 The signal yields are estimated by fitting the M_{bc} distributions. The fit function for the signal
 136 and peaking background components is constructed in the same way as in Ref. [26]. From the yield
 137 N of a specific decay mode, the corresponding dressed cross section is calculated as

$$\sigma^{\text{dressed}} = \frac{N}{(1 + \delta_{ISR})L\epsilon}$$

138 where $(1 + \delta_{ISR})$ is the radiative correction factor, L is the integrated luminosity and ϵ is the
 139 reconstruction efficiency. We fit simultaneously the energy dependence of the $e^+e^- \rightarrow B\bar{B}$,
 140 $e^+e^- \rightarrow B\bar{B}^*$, and $e^+e^- \rightarrow B^*\bar{B}^*$ cross sections and of the total $e^+e^- \rightarrow b\bar{b}$ cross section. The
 141 results are shown in Fig. 6 right, where the previous measurements from Belle are included.

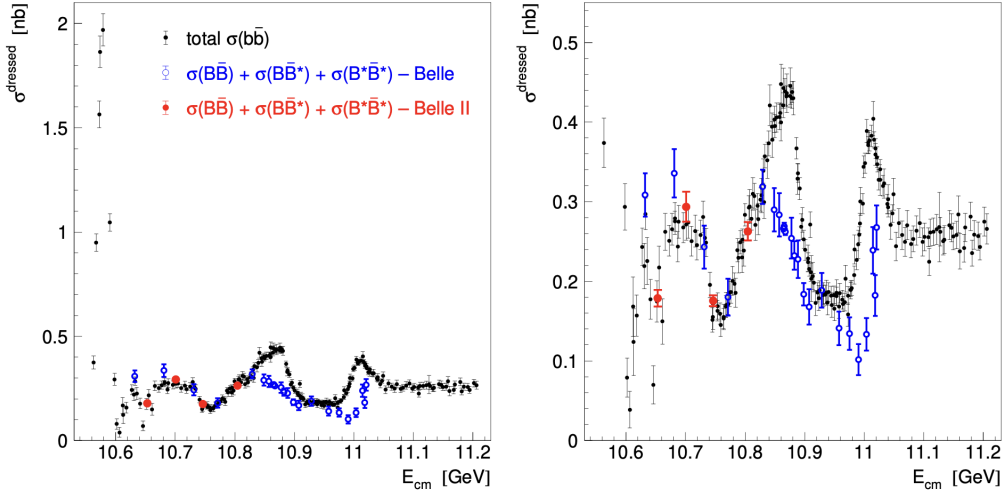


Figure 7: Energy dependence of the total $b\bar{b}$ dressed cross section obtained in Ref. [2] from the visible cross sections measured by Belle [28], and BaBar [27] (black circles) and the sum of the exclusive $B\bar{B}$, $B\bar{B}^*$, and $B^*\bar{B}^*$ cross sections measured by Belle [26] (open blue circles) and in this work (filled red circles). The right panel shows the low cross-section region with an expanded scale.

142 In Fig. 7 we show the sum of the exclusive $B\bar{B}$, $B\bar{B}^*$, and $B^*\bar{B}^*$ cross sections measured in
 143 this work and in the Belle experiment [26], superimposed on the total $b\bar{b}$ dressed cross section [2].
 144 The sum of measurements performed in this work agrees well with the total cross section. The
 145 deviation at higher energy is presumably due to the contribution of B_s^0 mesons, multibody final
 146 states $B^{(*)}\bar{B}^{(*)}\pi(\pi)$, and production of bottomonia in association with light hadrons.

147 4. Summary

148 We have shown recent measurements performed by the Belle II collaboration using the data
 149 set collected in an energy scan above the $\Upsilon(4S)$ resonance. These results are of great importance in
 150 understanding the nature of the new $\Upsilon(10753)$ state and, more generally, of the bottomonium(-like)

151 states above the open flavor threshold. The present status of the $\Upsilon(10753)$ is shown in Fig. 8. The
 152 uniqueness of the data set collected at center-of-mass energies around 10.75 GeV will enable Belle
 II to provide further unprecedented results in the quarkonium sector in the near future.

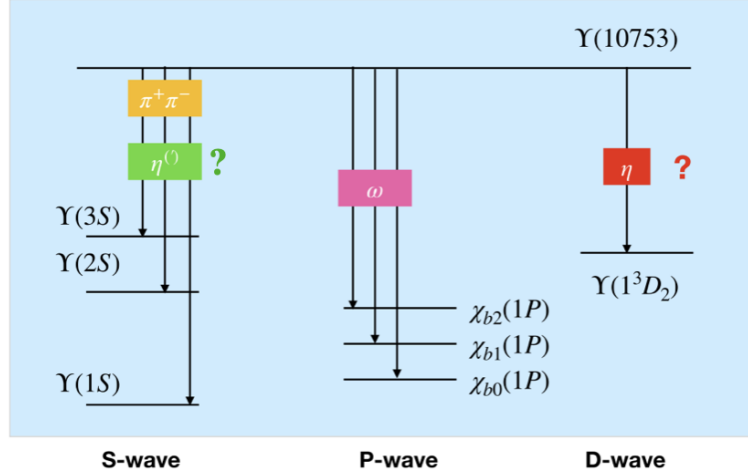


Figure 8: Present status of $\Upsilon(10753)$ state.

153

154 References

- 155 [1] R. Mizuk *et al.* (Belle Collaboration), *J. High Energy Phys.* **10** (2019) 220.
 156 [2] X. K. Dong, X. H. Mo, P. Wang, and C. Z. Yuan, *Chin. Phys. C* **44** (2020) 083001.
 157 [3] J. F. Giron and R. F. Lebed, *Phys. Rev. D* **102** (2020) 014036.
 158 [4] B. Chen, A. L. Zhang, and J. He, *Phys. Rev. D* **101** (2020) 014020.
 159 [5] Q. Li, M. S. Liu, Q. F. Lü, L. C. Gui, and X. H. Zhong, *Eur. Phys. J. C* **80** (2020) 59.
 160 [6] W. H. Liang, N. Ikeno, and E. Oset, *Phys. Lett. B* **803** (2020) 135340.
 161 [7] Y. S. Li, Z. Y. Bai, Q. Huang, and X. Liu, *Phys. Rev. D* **104** (2021) 034036.
 162 [8] Z. Y. Bai, Y. S. Li, Q. Huang, X. Liu, and T. Matsuki, *Phys. Rev. D* **105** (2022) 074007.
 163 [9] N. Hüsken, R. E. Mitchell, and E. S. Swanson, *Phys. Rev. D* **106** (2022) 094013.
 164 [10] V. Kher, R. Chaturvedi, N. Devlani, and A. K. Rai, *Eur. Phys. J. Plus* **137** (2022) 357.
 165 [11] N. Brambilla, W. K. Lai, J. Segovia, J. T. Castellà, and A. Vairo, *Phys. Rev. D* **99** (2019)
 166 014017.
 167 [12] P. Bicudo, N. Cardoso, L. Müller, and M. Wagner, *Phys. Rev. D* **103** (2021) 074507.

- 168 [13] Z. G. Wang, *Chin. Phys. C* **43** (2019) 123102.
- 169 [14] A. Ali, L. Maiani, A. Y. Parkhomenko, and W. Wang, *Phys. Lett. B* **802** (2020) 135217.
- 170 [15] N. A. Tornqvist, *Z. Phys. C* **61** (1994) 525.
- 171 [16] F. K. Guo, C. H. Duque, J. Nieves, and M. P. Valderrama, *Phys. Rev. D* **88** (2013) 054007.
- 172 [17] M. Karliner and S. Nussinov, *J. High Energy Phys.* **07** (2013) 153.
- 173 [18] D. Ebert, R. N. Faustov, and V. O. Galkin, *Phys. Lett. B* **634** (2006) 214.
- 174 [19] D. Ebert, R. N. Faustov, and V. O. Galkin, *Mod. Phys. Lett.* **24A** (2009) 567.
- 175 [20] A. Ali, C. Hambrock, I. Ahmed, and M. J. Aslam, *Phys. Lett. B* **684** (2010) 28.
- 176 [21] F. K. Guo, Ulf-G. Meißner, and C. P. Shen, *Phys. Lett. B* **738** (2014) 172.
- 177 [22] X. H. He *et al.* (Belle Collaboration), *Phys. Rev. Lett.* **113** (2014) 142001.
- 178 [23] I. Adachi *et al.* (Belle II Collaboration), *Phys. Rev. Lett.* **130** (2023) 091902.
- 179 [24] S. Liu, Z. Cai, Z. Jia, G. Li and J. Xie, arXiv:2312.02761563.
- 180 [25] M. Ablikim *et al.* (BESIII Collaboration), *Phys. Rev. D* **99** (2019) 091103.
- 181 [26] R. Mizuk *et al.* (Belle Collaboration), *J. High Energy Phys.* **06** (2021) 137.
- 182 [27] B. Aubert *et al.* (BaBar Collaboration), *Phys. Rev. Lett.* **102** (2009) 012001.
- 183 [28] D. Santel *et al.* (Belle Collaboration), *Phys. Rev. D* **93** (2016) 011101.